Model-based investigation into atmospheric freeze-drying assisted by power ultrasound.

JOURNAL OF FOOD ENGINEERING [ISSN: 0260-8774], 2015, 151, 7-15.

DOI: 10.1016/J.JFOODENG.2014.11.013

MODEL-BASED INVESTIGATION INTO ATMOSPHERIC FREEZE DRYING ASSISTED BY POWER ULTRASOUND

J.V. Santacatalina[1], D. Fissore[2], J.A. Cárcel[1], A. Mulet[1] and J.V. García-Pérez[1]*

[1]Grupo ASPA, Departamento de Tecnología de Alimentos, Universitat Politècnica de València, Camí de Vera s/n, E46022, València, Spain.

[2]Dipartimento di Scienza Applicata e Tecnologia, Politecnico di Torino, corso Duca degli Abruzzi 24, 10129 Torino, Italy.

*Corresponding author. Tel.: +34 963879376; fax: +34 963879839. E-mail address: jogarpe4@tal.upv.es (J.V. García-Pérez).

Abstract

Atmospheric freeze drying consists of a convective drying process using air at a temperature below the freezing point of the processed product, and with a very low relative humidity content. This paper focuses on the use of a simple one-dimensional model considering moving boundary vapor diffusion to describe the ultrasonic assisted atmospheric freeze-drying of foodstuffs. The case study is the drying of apple cubes (8.8 mm) at different air velocities (1, 2, 4 and 6 m/s), temperatures (-5, -10 and -15ºC), without and with (25, 50 and 75 W) power ultrasound application. By fitting the proposed diffusion model to the experimental drying kinetics, the effective diffusivity of water vapor in the dried product was estimated. The model was successfully validated by drying apple samples of different size and geometry (cubes and cylinders). Finally, a 2^3 factorial design of experiments revealed that the most relevant operating parameter affecting the drying time was the applied ultrasound power level.

Keywords:

Atmospheric freeze-drying, ultrasound, modeling, optimization.

1. Introduction

Atmospheric freeze drying (AFD) consists of a convective drying process where the temperature of the air has to be kept below the freezing point of the processed material, and the relative humidity has to be, in general, very low. Since the air is not saturated with water vapor, a vapor partial pressure gradient is created between the product and the air, forcing the ice to sublimate and the water vapor to diffuse to the air (Meryman, 1959; Bantle & Eikevik, 2011). AFD is generally carried out at temperatures of between -10ºC and the initial freezing point of the product, as this appears to be a good compromise between costs and final product quality (Wolff & Gibert, 1990a, 1990b; Claussen et al., 2007a, 2007b). The advantages of AFD are its lower cost compared to vacuum freeze drying and the possibility of its being carried out as a continuous process, thus also allowing energy recovery (Bantle et al., 2011)

In cold regions, the AFD process has a long history of use as a means of food preservation (Rhamann & Mujumdar, 2008a), although Meryman (1959) was the first to report the potential of AFD. Stawczyk et al. (2007) investigated the freeze-drying kinetics and the product quality of apple cubes in a fully automated heat pump-assisted drying system. Their results showed that the rehydration kinetics and the hygroscopic properties of the product were similar to those obtained by vacuum freeze drying. These findings agreed with the work of Claussen et al. (2007c), which was carried out using heat pump fluidized bed and tunnel dryers. However, despite the promises of low energy consumption and a better quality product, certain problems still exist in the atmospheric freeze-drying process, limiting its practical implementation. Furthermore, due to the low vapor diffusivity at atmospheric pressure, AFD is controlled by the internal resistance to heat and mass transfer, making it a long drying process (Rhamann & Mujumdar, 2008b).

Since the main drawback of the AFD process is the low sublimation rate, improving mass transfer would be beneficial. In the last few years, new power transducers with

extensive surface radiators have been developed for applications in gas media (Gallego-Juárez et al., 2001), such as de-foaming and air drying. Thus, high-intensity airborne ultrasound application brings about mechanical effects when the sound wave is directed into the product (Bhaskaracharya et al., 2009), which intensify the drying of foodstuffs (Gallego-Juarez et al., 2007; Gallego-Juarez, 2010; Riera et al., 2011). Therefore, high-intensity airborne ultrasound was suggested as a potential technology for improving mass transfer in AFD by Cárcel et al. (2011). Ozuna et al. (2014) and García-Perez et al. (2012) have also shown the feasibility of employing power ultrasound to accelerate the drying kinetics of fruits, vegetables and fish at low temperatures. The latter have achieved a maximum drying time reduction of 77% by applying power ultrasound during the drying of apple at -10ºC.

Mathematical modeling represents an important tool in the analysis of the drying process and the operation of the dryer (Mulet et al., 2010). Several empirical, semi-empirical, and analytical equations have been reported for predicting the drying curves for different products and operating conditions. However, there are few first principle models which have been reported to thoroughly describe the AFD process and even less effort has been made to assess its adequacy. One of these models is based on the Lewis equation and its accuracy depends greatly on the accurate evaluation of the thermal properties in the structure of the dried product (Claussen et al., 2007b). Rahman et al. (2009) also suggested a method based on the thermal properties of the product and used the analogy between Nusselt and Sherwood numbers to predict the drying rate in AFD. A similar approach was taken by Li et al. (2007), where a CFD model for an AFD process of apple was developed. When also working on the AFD of apple cubes, Stawczyk et al. (2007) observed that no first drying stage or constant drying rate occurred, and the complete dehydration process was controlled by internal water diffusivity. A similar conclusion was also drawn by Di Matteo et al. (2003). An analytical solution for AFD is presented by Wolff & Gibert (1990a, 1990b) where the

‘‘Uniformly Retreating Ice Front’’ (URIF) approach is coupled to the laws of heat and mass transfer. In the URIF model, the product is divided into two layers; a frozen (or wet) inner core and an outer dry layer. It is assumed that the drying occurs as a consequence of the frozen core gradually shrinking down to zero. Heat is transported from the surface of the product, causing sublimation at the ice front. The resulting water vapor is transported back to the surface and to the gas medium.

In this context, the main goals of this work were to evaluate the feasibility of a simple one-dimensional model to describe the ultrasonic assisted AFD process of apple cubes, as well as to validate such a model in different operating conditions. Finally, a suitable design of experiments coupled with the analysis of the effects was used to point out the key parameter for the atmospheric freeze drying process, which would positively contribute to further optimization stages.

2. Materials and methods

2.1. Raw material

Apples (*Malus domestica* cv. Granny Smith) were purchased in a local market (Valencia, Spain). Fruits were selected to obtain a homogeneous batch in terms of ripeness, size and color, and held at 4ºC until processing. Cubic samples (8.8 mm and 17.5 mm side) were obtained from the flesh using a household tool. Cylindrical samples (height 40 mm and diameter 15 mm) were also prepared using a 15 mm hole puncher. All the samples were wrapped in plastic film and frozen at -18±1ºC until processing (at least 24 h). The initial moisture content was measured by placing the samples in a vacuum oven at 70ºC and 200 mmHg until constant weight was reached, following the standard method 934.06 (AOAC, 1997).

2.2. Drying experiments

Drying experiments were carried out in a convective drier with air recirculation (Figure 1), already described in the literature (García-Pérez et al., 2012). The drier provides an automatic temperature and air velocity control. A cylindrical radiator (internal diameter 100 mm, height 310 mm, thickness 10 mm) driven by a power ultrasonic transducer (frequency 22 kHz, power capacity 90 W) was used as the drying chamber. The transducer generates an ultrasonic field inside the cylinder, which interacts with the samples and the surrounding air during drying. Air goes through the cylindrical radiator where samples were randomly placed in a holder for assuring a uniform treatment of them for both air flow and ultrasound application. A set of experiments was carried out to determine the drying kinetics of apple cubes (8.8 mm) at different air velocities (1, 2, 4 and 6 m/s), temperatures (-5, -10 and -15ºC), without and with (25, 50 and 75 W) power ultrasound (US) application. Another set of experiments was carried out with larger apple cubes (17.5 mm). In this case, the drying conditions used were -10ºC, 2 m/s and without US application.

In every experiment, the samples were weighed at preset times and the relative air humidity was kept at under 15±5%. For each run, the initial mass load density was 9.5 kg/m^3. The drying experiments were extended until the samples lost 80% of the initial weight. Every condition was tested in triplicate, at least.

Finally, a third drying test was carried out using apple cylinders, whose surface was kept isolated with a plastic film, with the exception of one of the flat surfaces. So, the water vapor outlet took place in only one direction. The samples were dried at -15°C, 2 m/s and without US application. In order to determine the moisture profile for different percentages of weight loss (10, 20, 30 and 40%), the cylinder was split into 5 equal sections and the individual moisture content of each section was determined following the standard method 934.06 (AOAC, 1997).

2.3. Mathematical modeling

As previously mentioned, the Uniformly Retreating Ice Front (URIF) model has been used to model the atmospheric freeze-drying of foodstuffs. Assuming cubic samples behave as spherical bodies (Figure 2A) during AFD, the mass balance for the water vapor in the dried product is given, in steady-state conditions, by the following equation:

$$\frac{d}{dr}\left(r^2 J_w\left(r\right)\right) = 0 \tag{1}$$

where the water flux is given by the well- known Fourier equation:

$$J_w\left(r\right) = -\frac{D_e M_w}{RT}\frac{dp_w\left(r\right)}{dr} \tag{2}$$

The integration of eq. (1), using eq. (2) and the following boundary conditions:

$$\begin{aligned} r &= L_0 - L_{dried} \qquad p_w = p_{w,i} \\ r &= L_0 \qquad\qquad\quad p_w = p_w^* \end{aligned} \tag{3}$$

gives:

$$p_w\left(r\right) = \frac{1}{r}\left(\frac{p_{w,i} - p_w^*}{L_{dried}}\right)L_0\left(L_0 - L_{dried}\right) + \left[p_w^* - \frac{1}{L_0}\left(\frac{p_{w,i} - p_w^*}{L_{dried}}\right)L_0\left(L_0 - L_{dried}\right)\right] \tag{4}$$

From eq. (4), it is possible to calculate the sublimation flux (using eq. (2)), thus obtaining:

$$J_w\left(r\right) = \frac{D_e M_w}{RT}\frac{1}{r^2}\left(\frac{p_{w,i} - p_w^*}{L_{dried}}\right)L_0\left(L_0 - L_{dried}\right) \tag{5}$$

and, finally, the sublimation flow rate:

$$G = 4\pi r^2 J_w\left(r\right) = \frac{D_e M_w}{RT}4\pi\frac{L_0\left(L_0 - L_{dried}\right)}{L_{dried}}\left(p_{w,i} - p_w^*\right) \tag{6}$$

The mass flow rate from the surface of the sample to the drying chamber is also given by the following equation: G

$$G = S\alpha \frac{M_w}{RT}\left(p_w^* - p_{w,c}\right) \tag{7}$$

Using eqs. (6) and (7) it is possible to calculate the sublimation flow rate in the following way:

$$G = \frac{M_w}{RT} \frac{1}{\frac{1}{S\alpha} + \frac{L_{dried}}{4\pi D_e L_0 (L_0 - L_{dried})}} \left(p_{w,i} - p_{w,c}\right) \tag{8}$$

where $p_{w,i}$, the partial pressure of water at the interface of sublimation is a well- known function of the temperature.

Following exactly the same approach, it is possible to calculate the heat flow rate in the dried layer by means of the following equation:

$$Q = \frac{1}{\frac{1}{S\beta} + \frac{L_{dried}}{4\pi\lambda_{dried} L_0 (L_0 - L_{dried})}} \left(T_{air} - T_i\right) \tag{9}$$

All the energy transferred into the product is used for ice sublimation and, thus:

$$Q = G\Delta H_s \tag{10}$$

Equation (10) can be used to calculate the interface temperature, given the values of the operating conditions, of the heat and mass transfer coefficients, of product parameters D_e and λ_{dried}, and of the dried layer thickness. Then, it is possible to calculate the sublimation flow rate (using eq. (8)) and the evolution of the dried volume:

$$\frac{dV_{dried}}{dt} = \frac{G}{\rho_{dried}\left(W_0 - W_f\right)} \tag{11}$$

and, finally, of the residual amount of ice in the sample:

$$-\frac{dW}{dt} = \rho_{dried}\left(W_0 - W_f\right)\frac{dV_{dried}}{dt} \tag{12}$$

In the case of planar geometry, as shown in Figure 2, graph B, exactly the same approach can be followed. Thus, the mass balance for the water vapor in the dried product is given, in steady-state conditions, by the following equation:

$$\frac{d}{dx}\left(J_w\left(x\right)\right)=0 \tag{13}$$

with the following boundary conditions:

$$\begin{aligned} x &= L_0 - L_{dried} \qquad p_w = p_{w,i} \\ x &= L_0 \qquad\qquad\quad p_w = p_w^* \end{aligned} \tag{14}$$

and the water flux is given by the Fourier equation:

$$J_w\left(x\right)=-\frac{D_e M_w}{RT}\frac{dp_w\left(x\right)}{dx} \tag{15}$$

After some calculations, it is possible to obtain the following equation to calculate the sublimation flow rate:

$$G=\frac{M_w}{RT}\frac{1}{\frac{1}{\alpha}+\frac{L_{dried}}{D_e}}\left(p_{w,i}-p_{w,c}\right) \tag{16}$$

and the heat flow rate in the dried layer is given by the following equation:

$$Q=\frac{1}{\frac{1}{\beta}+\frac{L_{dried}}{\lambda_{dried}}}\left(T_{air}-T_i\right) \tag{17}$$

In this case, it is also possible to assume that all the energy transferred into the product is used for ice sublimation, i.e. eq. (10) and, thus calculating the interface temperature from the values of the operating conditions, heat and mass transfer coefficients, product parameters D_e and λ_{dried}, and dried layer thickness. Then, the sublimation flow rate (using eq. (16)) and the evolution of the dried layer thickness can be estimated:

$$\frac{dL_{dried}}{dt}=\frac{G}{\rho_{dried}S(W_0-W_f)} \tag{18}$$

and, finally, of the residual amount of ice in the sample:

$$-\frac{dW}{dt} = S\rho_{dried}(W_0 - W_f)\frac{dL_{dried}}{dt} \quad (19)$$

As regards the estimation of heat and mass transfer coefficients, α and β, several equations can be found in the literature. Among others, Krokida et al. (2002) reported various empirical equations with which to calculate the coefficient β, given as a function of the air Reynolds number:

$$j_h = aRe^n \quad (20)$$

while the Lewis equation is used to calculate the coefficient α:

$$\alpha = \frac{\beta}{\rho_{air} c_{p,air}} \quad (21)$$

In any case, the atmospheric freeze-drying process appears to be controlled by the internal resistance to water vapor transfer in most cases, as is also reported by Bantle et al. (2011) for the AFD process of peas, and as also pointed out in this study for apple drying; thus, the correlations used to calculate α and β do not significantly affect the accuracy of the results. The constant parameters used in the AFD modeling of apple cubes and cylinders are included in Table 1.

2.4. Design of experiments

In order to assess the effect of the various operating parameters, namely air temperature, air velocity and ultrasound application, on drying time, a standard Design of Experiments (DoE) technique was used. This aims to investigate the reciprocal interactions among the variables, and to find those which play the major role in the drying kinetics (Montgomery, 2005). In particular, a 2^3 factorial design of experiments was used to evaluate how air temperature (factor A), air velocity (factor B), and acoustic power (factor C) affect the drying time. High (+) and low (-) values of these

parameters (factor A: -10 and -5°C, factor B: 2 and 6 m/s and factor C: 0 and 50 W) were considered, as is graphically illustrated in Figure 3, where these eight combinations are represented by lowercase letters of the alphabet. Lowercase letters indicate that the parameter is at the high level, for the sake of clarity: a identifies the combination of A at the high level (-5°C) and B and C at the low level (2 m/s and 0 W), ab identifies the combination of A and B at the high level (-5°C and 6 m/s) and C at the low level (0 W), abc identifies the combination of A, B and C at the high level (-5°C, 6 m/s, 50 W) while (1) identifies the combination of A, B and C at the low level (-10°C, 2 m/s and 0 W). Then, the single effects of various parameters can be calculated. For example, the effects of A are:

- $\left[a-(1)\right]/n$ when the values of B and C are both low;

- $\left[ab-b\right]/n$ when the value of B is high and the value of C low;

- $\left[ac-c\right]/n$ when the value of C is high and the value of B low and

- $\left[abc-bc\right]/n$ when the values of B and C are both high,

where n is the number of repetitions of the test. By averaging the previously calculated single effects, the total effect of A, also known as the contrast parameter, on the drying time is obtained:

$$A=\frac{1}{4n}\left[a-(1)+ab-b+ac-c+abc-bc\right]=\frac{Contrast_A}{4n} \tag{22}$$

Similarly, the effects of parameters B and C can be calculated, as well as the interactions between these factors. The effect can be positive or negative: if the value is positive, when the parameter increases (from the minimum to the maximum) the observed variable (the drying time) also increases, and vice versa when the value is negative. Finally, the percentage contribution of each factor to the drying time can be determined. The analysis of variance “ANOVA” was carried out using the Fisher test to

verify the significance of the differences between the arithmetic means of the various groups.

3. Results and discussion

3.1. Assessment of model adequacy and water diffusivity estimation

The drying kinetics of apple cubes (8.8 mm side) processed at different velocities (1, 2, 4 and 6 m/s), temperatures (-15, -10 and -5°C), and without and with (25, 50 and 75 W) power ultrasound application were modeled using the equations described in the previous sections. For modeling purposes, a spherical geometry has been assumed for the food samples, and the sphere diameter has been determined in such a way that the product volume is the same as that of the cubic samples. The value of water effective diffusivity in the dried product (D_e) has been determined by looking for the best fit between the calculated and measured values of the residual moisture in the product vs time.

For every combination of the operating conditions under investigation, the model was observed to fit the experimental data very well, as can be observed in Figure 4. Claussen et al. (2007b) also used the URIF model to simulate the AFD of apple, turnip, cabbage and cod pieces, exhibiting a good agreement with the experimental data (not shown), whereas Li et al. (2007) found some differences between the experimental values and those calculated by means of the URIF model at the beginning of the AFD of apple cubes. Using the same approach, Reyes et al. (2010) reported a 10% deviation of the model for the AFD of berries.

As regards the values of the water vapor effective diffusivity in the dried product, this study permitted the effect of the different operating parameters (temperature, air velocity and applied acoustic power) on D_e and, thus, on drying kinetics to be demonstrated. Air temperature was observed to have a significant ($p<0.05$) effect on

the identified D_e (Table 2): the higher the temperature used, the higher the D_e value. This influence of temperature was also observed in the US-assisted experiments. As for the effect of air velocity, as expected, it has no effect on the estimated value of D_e (Table 3) when US is not applied. Otherwise, for drying experiments conducted with US application, a slightly lower D_e was identified for the experiments carried out at the highest air velocities tested (4 and 6 m/s); however, no significant ($p<0.05$) differences were observed. This fact could be due to some disruption of the ultrasonic field caused by the turbulences produced by high air flow velocities, reducing the acoustic intensity that reaches the sample, as reported by García-Pérez et al. (2006). Low air flow rates should not affect the ultrasonic field, thus a major fraction of ultrasonic energy would be available to increase water vapor diffusivity into the sample. In every case, the obtained D_e values were much higher (6 orders of magnitude) than those computed by Santacatalina et al. (2014) and Li et al. (2008) for AFD apple kinetics when using a strict diffusion model and identifying the liquid water diffusivity.

As regards the US application, the increase in the level of applied acoustic power led to a rise in the effective diffusivity (Table 4). It should also be remarked that the lowest power tested (25 W) allowed a huge increase (370%) in the D_e value to be obtained (Table 4). Therefore, it is illustrated that US application is very effective at accelerating the AFD experiments, even when using a low acoustic power. Several effects of ultrasonic waves to improve mass diffusion in solid matrix have been reported (Gallego-Juárez, 1998). In this sense, US produce series of cyclical and rapid (>20 kHz) compressions and expansions, a mechanism known as sponge effect; this alternating stress creates microscopic channels that help to make the movement of water vapor from the ice front towards the product surface easier. In addition, ultrasound may also contribute to the water sublimation since, to a certain extent, the attenuation of the acoustic wave may provide the energy needed for the water to change state (Gallego-Juárez, 2010).

The obtained results are interesting because, just by using a low acoustic power, the amount of energy consumed by an AFD experiment could be reduced (due to the shorter drying time) and the degradation of the structure of the sample could be minimal. In this sense, Puig et al. (2012) have analyzed the microstructure of eggplant and how it is affected by the application of US during its drying at 40ºC and have reported that the lowest acoustic power tested (45 W) provoked less degradation than when US was applied at its maximum power capacity (90 W).

3.2. Model validation

A first attempt to validate the model consisted of using the diffusivities identified for each one of the drying conditions tested to predict the drying times and compare them to the experimental times. Since the air velocity did not have a significant effect on the value of the diffusivity for the experiments conducted without US application, an average D_e value was used to simulate the drying kinetics at the four air velocities tested so it could be further compared to the experimental results (Figure 5). It may be observed that the experimental and calculated times were very similar for every condition tested.

Moreover, a more rigorous model validation was addressed by carrying out additional experiments to those used to identify the diffusivity values. Thus, the diffusivity value obtained in the experiments performed on apple cubes of 8.8 mm side (at -10°C, 2 m/s and without US application) to model a drying experiment carried out under the same drying conditions, but on different-sized samples: cubes of 17.6 mm side. As can be observed in Figure 6, experimental data were quite similar to those simulated.

Model validation was also performed with a third set of experiments under completely different experimental conditions. In this case, atmospheric freeze drying experiments were carried out on apple cylinders, 40 mm in height and 15 mm in diameter, which

were water-proof isolated to behave as infinite slabs of 40 mm, as already mentioned in section 2.2. The D_e obtained from the experiments performed on apple cubes (8.8 mm side) under the same experimental conditions (2 m/s, -15°C, without US application) was used to model apple cylinder experiments. The evolution of the moisture profile was calculated using the model, taking into account the position of the sublimation front at every time in order to estimate the moisture of each one of the five sections of apple cylinders. Figure 7 depicts the reasonably good match between the experimental moisture of the sections and the computed value. Therefore, the moisture profile in the samples confirmed the assumptions considered in the model, as well as the results obtained. In Figure 7, it may be seen how the sublimation front moves from the surface of the sample in contact with the air, leaving a dry layer through which water vapor diffuses onto the surface. Meanwhile, the frozen area maintained the initial moisture content ($W/W_0 = 1$) and shrank as drying progressed. These retreating ice fronts have also been observed by Crespi et al. (2008) when analyzing paper samples that had previously been soaked in distilled water and freeze-dried for different times by immersing the partially dried sample in a dye that colored the ice (wet zone). However, as far as we are concerned, the experimental validation of the URIF model showing the location of the ice front has not been reported for foodstuffs.

3.3. Analysis of the effects

The process variables considered in this study were temperature, air velocity and ultrasound application. In order to quantify the effect of these operating variables on the AFD times, a set of experiments was performed. Two levels (high and low) of each variable were selected to make a two-level factorial design (2^3), with three replicates from each run. The contribution percentages of each factor to the drying time and their interactions are shown in Figure 8. It can be observed that the variable with the most relevant effect on the drying time was US application, followed by temperature and the

interaction between them. The effect of air velocity appears to be negligible under these drying conditions, as has previously been mentioned. Therefore, for the drying conditions studied in this design, the key parameter is US application. Consequently, this parameter should be conveniently modified to optimize the drying process.

4. Conclusions

In this study, a simple one-dimensional model has been successfully applied to assess the effect of the US application on the AFD kinetics of apple. US severely shortened the drying time under every condition tested. On the other hand, the model has been validated under different drying conditions (different size and geometry of the sample) obtaining a good fit to the experimental data and showing the retreat of the ice front during AFD. From a 2^3 factorial design of experiments, it has been proven that US application is the parameter with the greatest influence on the AFD time and, consequently, is the key factor for the further optimization of the process.

Acknowledgements

The authors acknowledge the financial support of the Spanish Ministerio de Economia y Competitividad (MINECO) and of the European Regional Development Fund (ERDF) through the project DPI2012-37466-CO3-03, the FPI fellowship (BES-2010-033460) and the EEBB-I-14-08572 fellowship granted to J.V. Santacatalina for a short stay at Politecnico di Torino.

List of symbols

S	surface of the product, m^2
a	parameter used to calculate the heat transfer coefficient

$c_{p,air}$	air specific heat, J/kg K
D_e	effective diffusivity of water vapor in the dried product, m^2/s
G	sublimation flow rate, kg/s
ΔH_s	heat of sublimation, J/kg
J_w	sublimation flux, kg/s m^2
j_h	*j-factor* for the heat transfer
L_0	initial characteristic dimension of the product, m
L_{dried}	characteristic dimension of the dried product, m
M_w	water molecular weight, kg/kmol
n	parameter used to calculate the heat transfer coefficient
p_w	water vapor partial pressure, Pa
$p_{w,c}$	water vapor partial pressure in the drying chamber, Pa
$p_{w,i}$	water vapor partial pressure at the sublimation interface, Pa
p_w^*	water vapor partial pressure at the external surface of the product, Pa
Q	heat flow rate, W
R	ideal gas constant, J/kmol K
Re	Reynolds number
r	radial coordinate
T	temperature, K
T_{air}	air temperature, K
T_i	temperature of the sublimation interface, K
t	time, s

V_{dried} volume of the dried product, m^3

W water content in the product, $kg_{water}/kg_{dry\ matter}$

W_0 water content in the product at the beginning of the drying process, $kg_{water}/kg_{dry\ matter}$

W_f water content in the product at the end of the drying process, $kg_{water}/kg_{dry\ matter}$

x axial coordinate, m

Greek letters

α mass transfer coefficient, m/s

β heat transfer coefficient, $W/m^2\ K$

λ_{dried} thermal conductivity of the dried product, W/m K

ρ_{air} density of the air, kg/m^3

ρ_{dried} density of the dried product, kg/m^3

References

Association of Official Analytical Chemists (AOAC) (1997). Official methods of analysis. Association of Official Analytical Chemists, Arlington, Virginia, USA.

Bantle, M., & Eikevik, T.M. (2011). Parametric study of high intensity ultrasound in the atmospheric freeze drying of peas. *Drying Technology, 29*, 1230-1239.

Bantle, M., Kolsaker, K., & Eikevik, T.M. (2011). Modification of the Weibull distribution for modeling atmospheric freeze-drying of food. *Drying Technology, 29*, 1161-1169.

Bhaskaracharya, R.K., Kentish, S., & Ashokkumar, M. (2009). Selected applications of ultrasonics in food processing. *Food Engineering Reviews, 1,* 31-49.

Cárcel, J.A., García-Pérez, J.V., Peña, R., Mulet, A., Riera, E., Acosta, V., & Gallego-Juárez, J.A. (2011). Procedimiento y dispositivo para mejorar la transferencia de materia en procesos a baja temperatura mediante el uso de ultrasonidos de elevada intensidad. International patent, Spanish ref. P201131512. Internacional PCT ref. 120120283, September 20.

Claussen, I.C., Ustad, T.S., Strømmen, I., & Walde, P.M. (2007a). Atmospheric freeze drying - A review. *Drying Technology, 25,* 957-967.

Claussen, I.C., Andresen, T., Eikevik, T.M., & Strømmen, I. (2007b). Atmospheric freeze drying - Modeling and simulation of a tunnel dryer. *Drying Technology, 25,* 1959-1965.

Claussen, I.C., Strømmen, I., Torstveit Hemmingsen, A.K., & Rustad, T. (2007c). Relationship of product structure, sorption characteristics, and freezing point of atmospheric freeze-dried foods. *Drying Technology, 25,* 853-865.

Crespi, E., Capolongo, A., Fissore, D., & Barresi, A. (2008). Experimental investigation of the recovery of soaked paper using evaporative freeze drying. *Drying Technology, 26,* 349-356.

Di Matteo, P., Donsì, G., & Ferrari, G. (2003). The role of heat and mass transfer phenomena in atmospheric freeze-drying of foods in a fluidized bed. *Journal of Food Engineering, 59,* 267-275.

Gallego-Juárez, J.A. (1998). Some applications of air-borne power ultrasound to food processing. In: *Ultrasound in Food Processing*, Povey, M.J.W., & Mason, T.J. Eds., Thomson Science, London, UK, 127-143.

Gallego-Juárez, J.A., Yang, T., Vázquez-Martínez, F., Gálvez-Moraleda, J.C., & Rodríguez-Corral, G. (2001). Dehydration method and device. US Patent, ref. 6233844 B1, May 22.

Gallego-Juárez, J.A., Riera, E., de la Fuente-Blanco, S., Rodríguez-Corral, G., Acosta-Aparicio, V.M., & Blanco, A. (2007). Application of high-power ultrasound for dehydration of vegetables: processes and devices. *Drying Technology, 25*, 1893-1901.

Gallego-Juárez, J.A. (2010). High-power ultrasonic processing: Recent developments and prospective advances. *Physics Procedia, 3*, 35-47.

García-Pérez, J.V., Cárcel, J.A., de La Fuente-blanco, S., & Riera-Franco de Sarabia, E. (2006). Ultrasonic drying of foodstuff in a fluidized bed: Parametric study. *Ultrasonics, 44,* e539-e543.

García-Pérez, J.V., Cárcel, J.A., Riera, E., Rosselló, C., & Mulet, A. (2012). Intensification of low temperature drying by using ultrasound. *Drying Technology, 30*, 1199-1208.

Krokida, M.K., Maroulis, Z.B., & Marinos-Kouris, D. (2002). Heat and mass transfer coefficients in drying: Compilation of literature data. *Drying Technology, 20,* 1-18.

Li, S., Stawczyk, J., & Zbicinski, I. (2007). CFD model of apple atmospheric freeze drying at low temperature. *Drying Technology, 25*, 1331-1339.

Li, S., Zbicinski, I., Wang, H., Stawczyk, J., & Zhang, Z. (2008). Diffusion model for apple cubes atmospheric freeze-drying with the effect of shrinkage. *International Journal of Food Engineering, 6*, 1-7.

Meryman, H.T. (1959). Sublimation: Freeze-drying without vacuum. *Science, 130,* 628-629.

Montgomery, D.C. (2005). *Design and analysis of experiments*, 7th ed., John Wiley and Sons, New York, USA.

Mulet, A., Cárcel, J.A., Sanjuán, N., & García-Pérez, J.V. (2010). Food dehydration under forced convection conditions. In: Recent Progress in Chemical Engineering, J. Delgado ed., Studium Press LLC, Houston, TX, USA.

Ozuna, C., Cárcel, J.A., Walde, P.M. & García-Pérez, J.V. (2014). Low-temperature drying of salted cod (Gadus morhua) assisted by high power ultrasound: Kinetics and physical properties. *Innovative Food Science and Emerging Technologies, 23*, 146-155.

Puig, A., Pérez-Munuera, I., Cárcel, J.A., Hernando, I., & García-Pérez, J.V. (2012). Moisture loss kinetics and microstructural changes in eggplant (Solanummelongena L.) during conventional and ultrasonically assisted convective drying. *Food and Bioprocess Processing, 90*, 624-632.

Rahman, S. (2009). A novel approach on atmospheric freeze drying. Lambert Academic Publishing, Köln, Germany.

Reyes, A., Bubnovich, V., Bustos, R., Vásquez, M., Vega, R., & Scheuermann, E. (2010). Comparative study of different process conditions of freeze drying of ‘‘Murtilla’’ berry. *DryingTechnology, 28,* 1416-1425.

Rhamann, S.M.A., & Mujumdar, A.S. (2008a). Vacuum and atmospheric freeze drying. In: *Guide to Industrial Drying - Principles, Equipments and New Developments,* Mujumdar, A.S., Ed., Colour Publications Ltd., Hyderabad, India.

Rhamann, S.M.A., & Mujumdar, A.S. (2008b). A novel atmospheric freeze-drying system using a vibro-fluidized bed with adsorbent. *DryingTechnology, 26,* 393-403.

Riera, E., García-Pérez, J.V., Acosta, V.M., Cárcel, J.A., & Gallego-Juárez, J.A. (2011). A computational study of ultrasound-assisted drying of food materials. In:

Multiphysics Simulation of Emerging Food Processing Technologies, Knoerzer, K., Juliano, P., Roupas, P., & Versteeg,C., Eds., IFT Press, Chicago, USA, 265-302.

Santacatalina, J.V., Rodríguez, O., Simal, S., Cárcel, J.A., Mulet, A., & García-Pérez, J.V. (2014). Ultrasonically enhanced low-temperature drying of apple: Influence on drying kinetics and antioxidant potential. *Journal of Food Engineering, 138,* 35-44.

Stawczyk, J., Li, S., Witrowa-Rajchert, D., & Fabisiak, A. (2007). Kinetics of atmospheric freeze-drying of apple. *Transport in porous media, 66,* 159-172.

Wolff, E., & Gibert, H. (1990a). Atmospheric freeze drying. Part 1: Design, experimental investigation and energy-saving advantages. *Drying Technology, 8,* 385-404.

Wolff, E., & Gibert, H. (1990b). Atmospheric freeze drying. Part 2: Modelling drying kinetics using adsorption isotherms. *Drying Technology, 8,* 405-428.

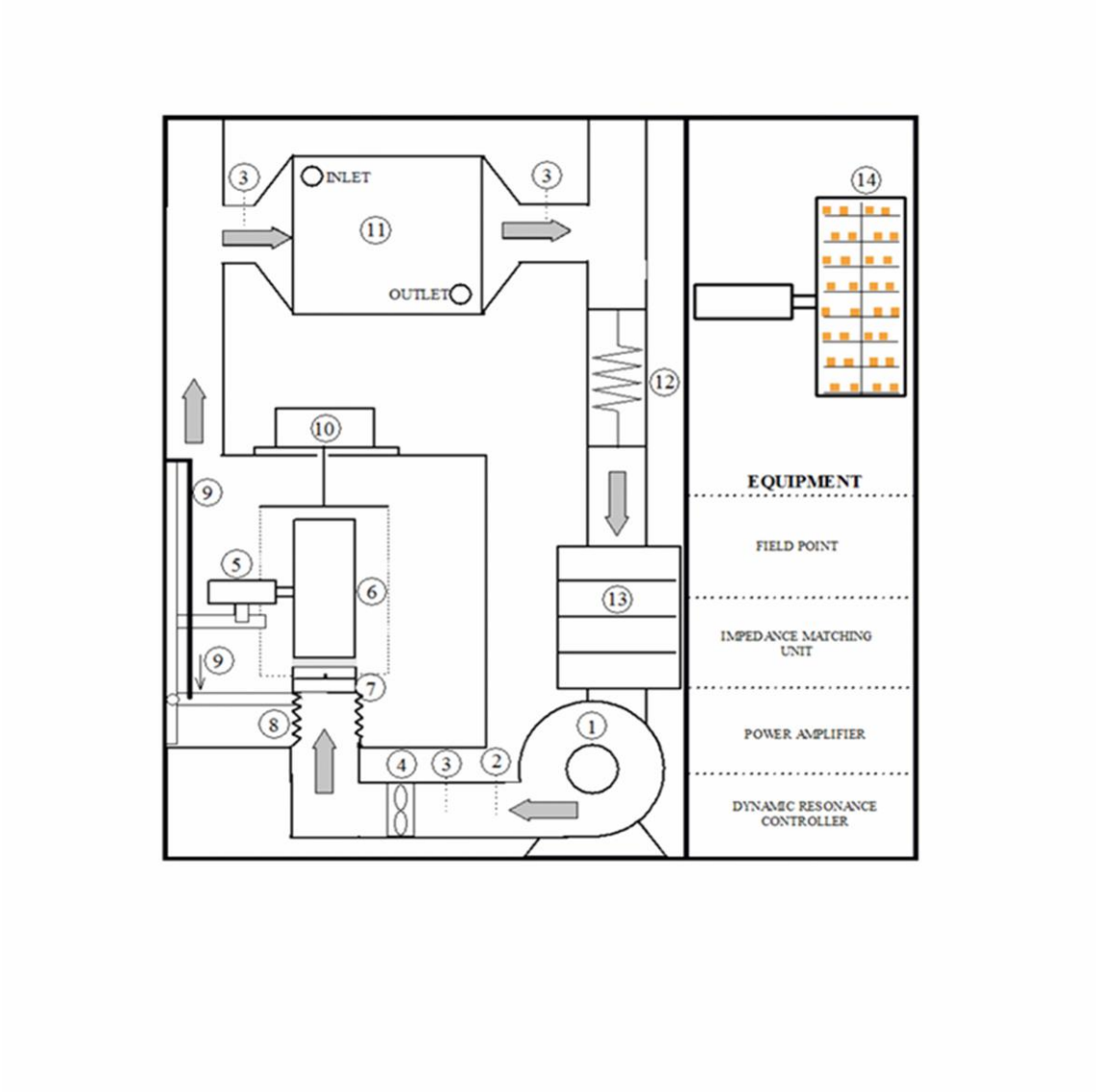

Figure 1. Scheme of the ultrasonically assisted convective drier: 1, fan; 2, Pt-100; 3, temperature and relative humidity sensor; 4, anemometer; 5, ultrasonic transducer; 6, vibrating cylinder; 7, sample load device; 8, retreating pipe; 9, slide actuator; 10, weighing module; 11, heat exchanger; 12, heating elements; 13, desiccant tray chamber; 14, details of the sample load on the trays.

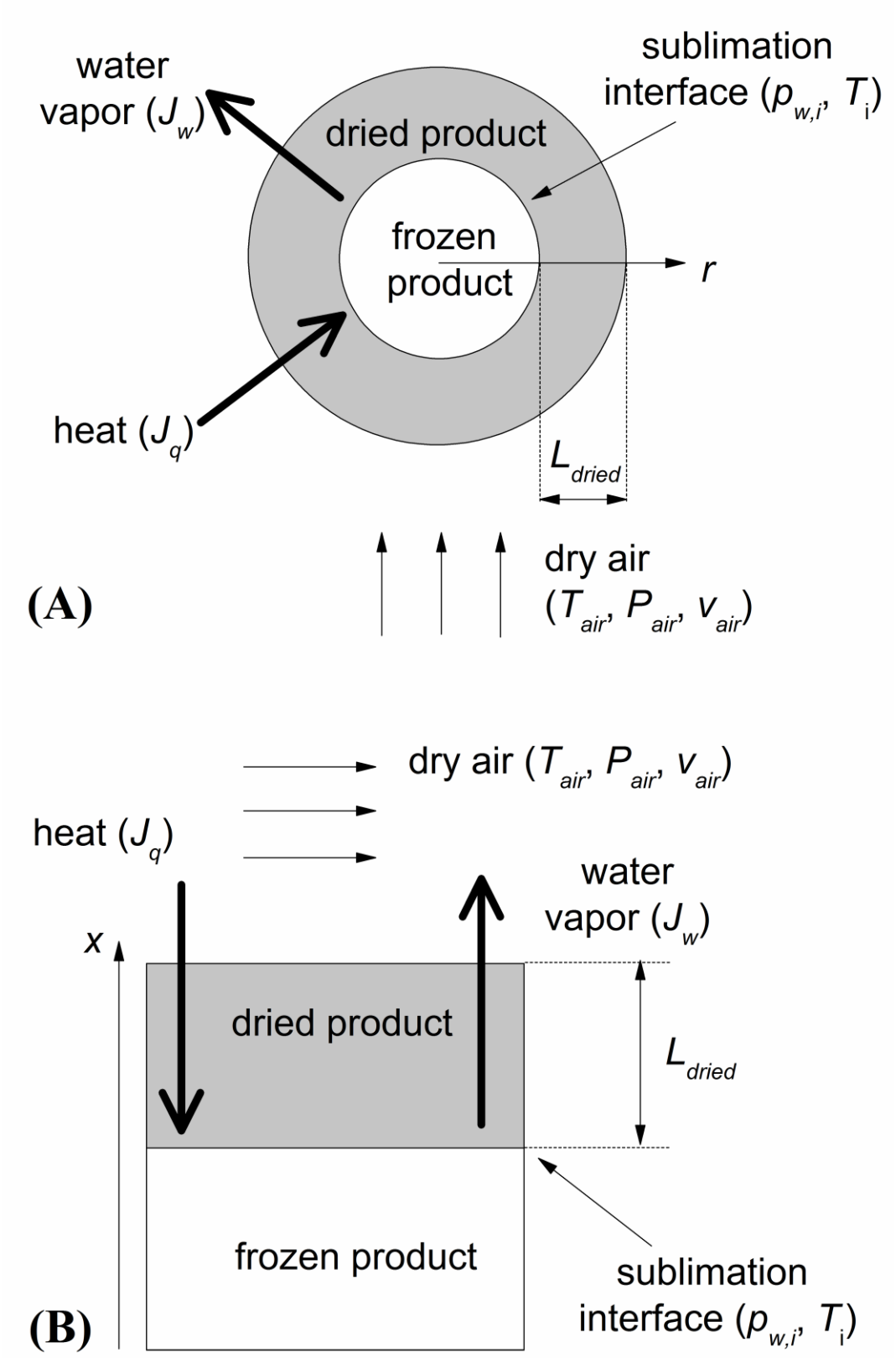

Figure 2. Sketch of a partially freeze-dried product with spherical (A) and planar (B) geometry.

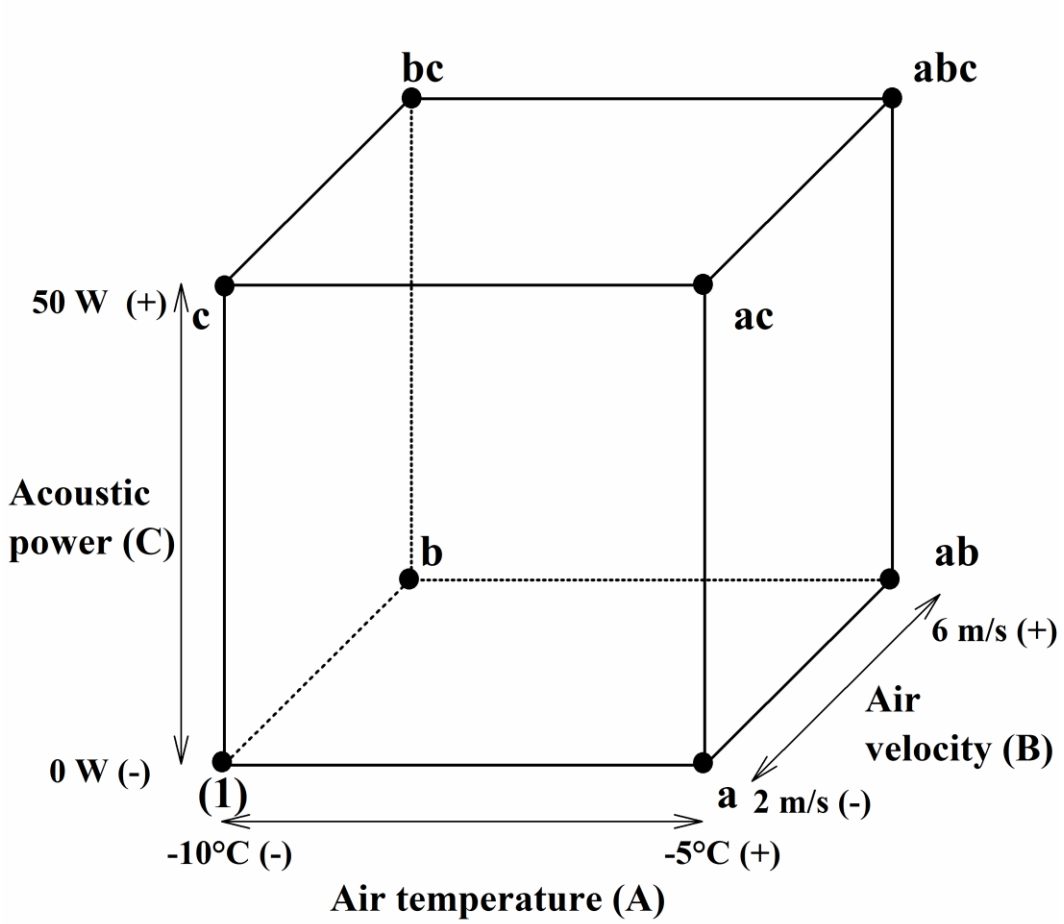

Figure 3. Graphical representation of the 2^3 factorial design used to investigate the effect of air temperature (A), of air velocity (B), and of ultrasonic application (C) on the drying time.

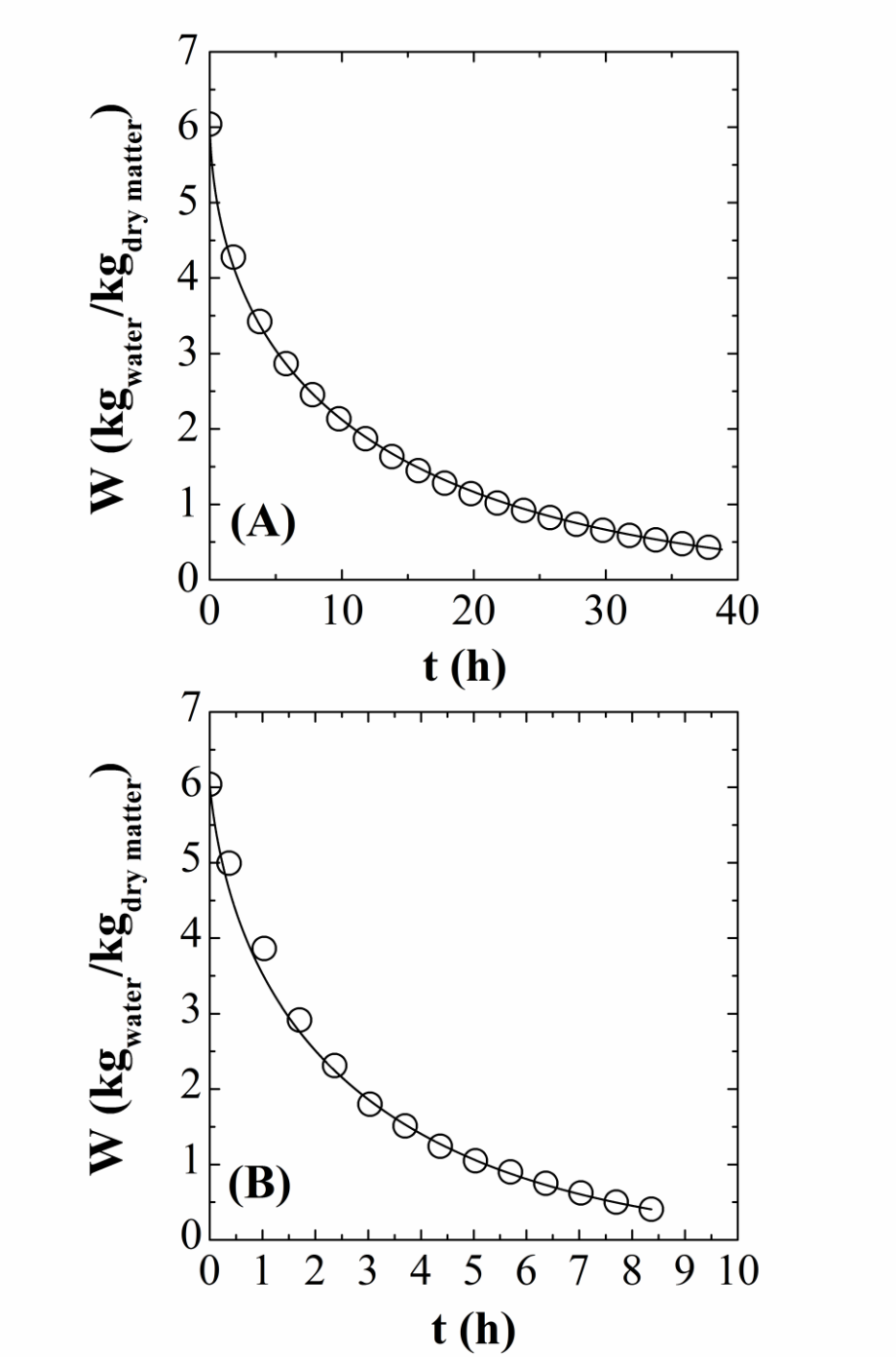

Figure 4. Comparison between the evolution of the residual amount of water in the product measured experimentally (symbols) and calculated using the mathematical model of the process (lines) during atmospheric freeze-drying of apple samples (air temperature: -10°C, air velocity: 2 m/s) without ultrasound (A) and with ultrasound application (50 W, B).

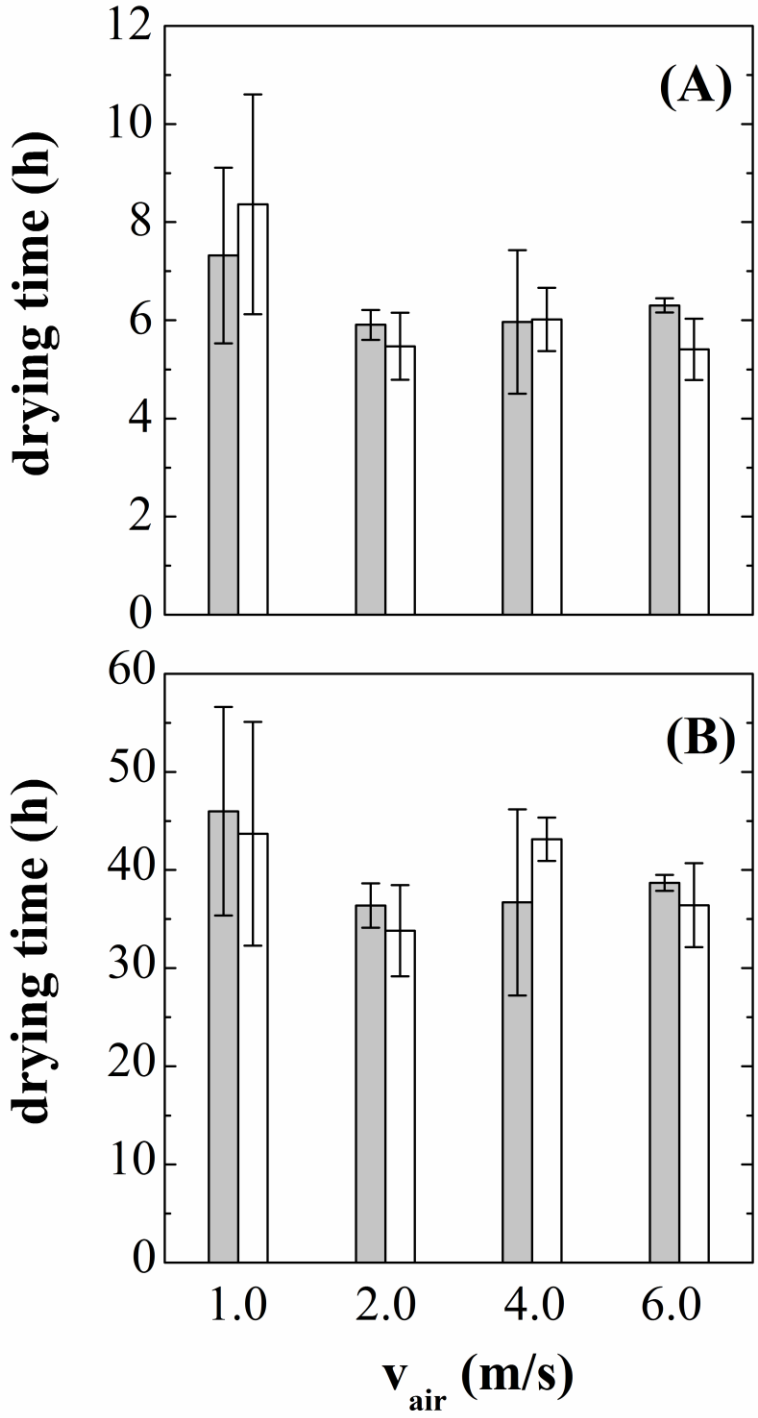

Figure 5. Comparison between the experimentally measured (empty bars) and the calculated (grey bars) values of the time required to reduce the amount of water in the sample by 50% (A) and by 90% (B) during atmospheric freeze-drying of apple samples as a function of air velocity (air temperature: -10°C), without ultrasound application.

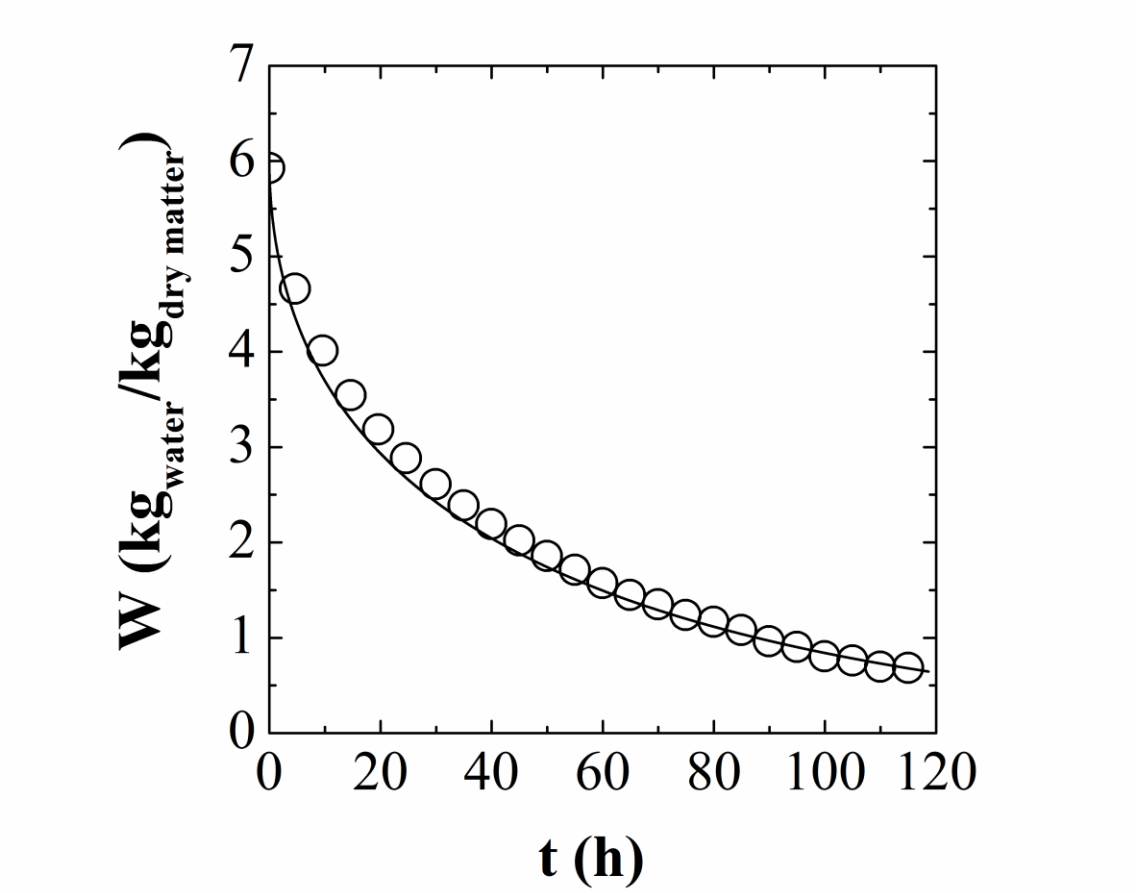

Figure 6. Comparison between the evolution of the residual amount of water in the product measured experimentally (symbols) and calculated using the mathematical model of the process (lines) during atmospheric freeze-drying of apple samples (17.6 mm side, air temperature: -10°C, air velocity: 2 m/s) without ultrasound application.

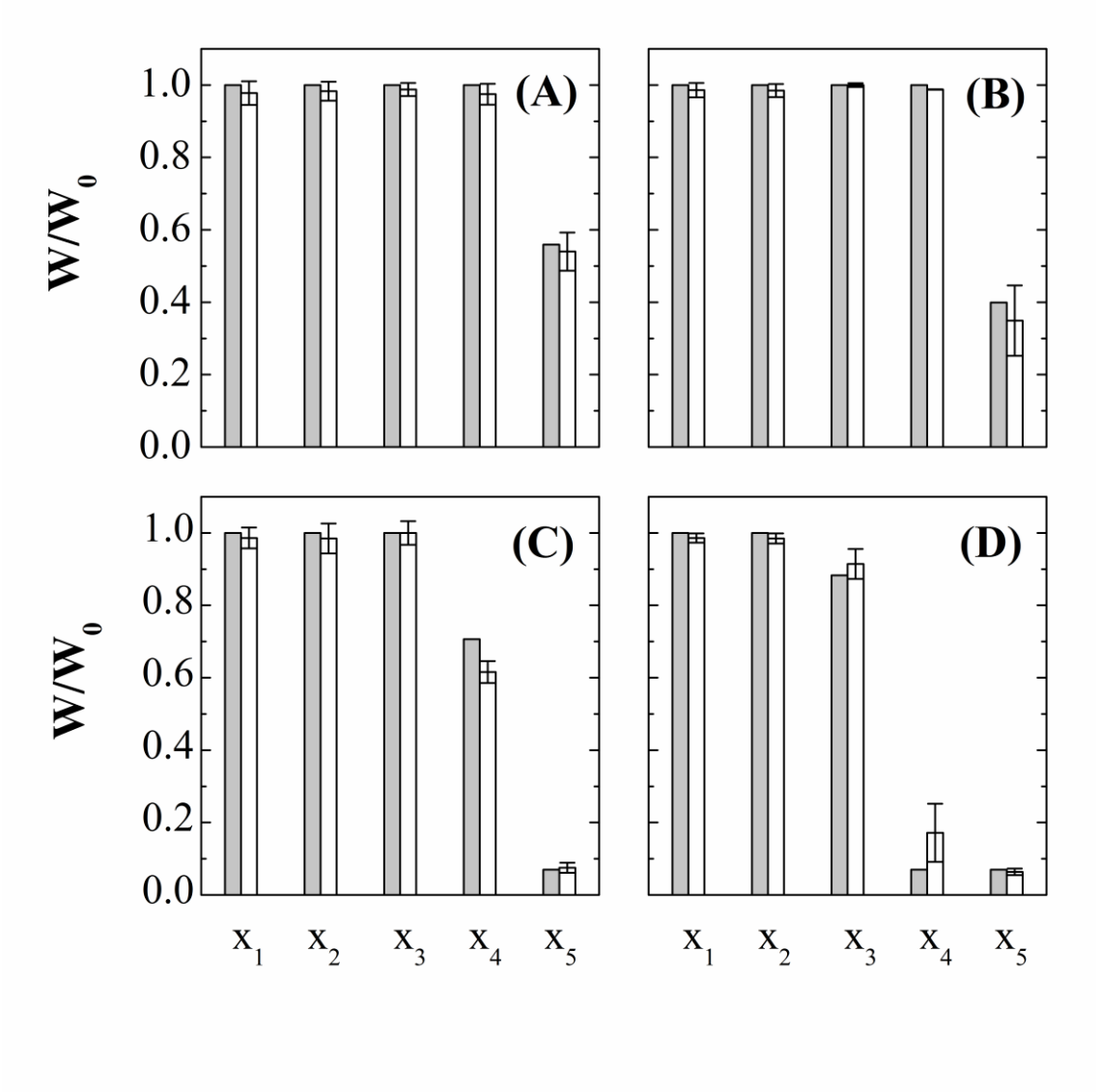

Figure 7. Comparison between the experimentally measured (empty bars) and the calculated (grey bars) values of the residual amount of water in the product at different axial positions (given as distance from the isolated flat surface; x_1 = 0.036 m, x_2 = 0.028 m, x_3 = 0.02 m, x_4 = 0.012 m, x_5 = 0.004 m) during atmospheric freeze-drying of apple samples (air temperature: -10°C, air velocity: 2 m/s, without ultrasound application), for different total weight loss (graph A: 10%, graph B: 20%, graph C: 30%, graph D: 40%).

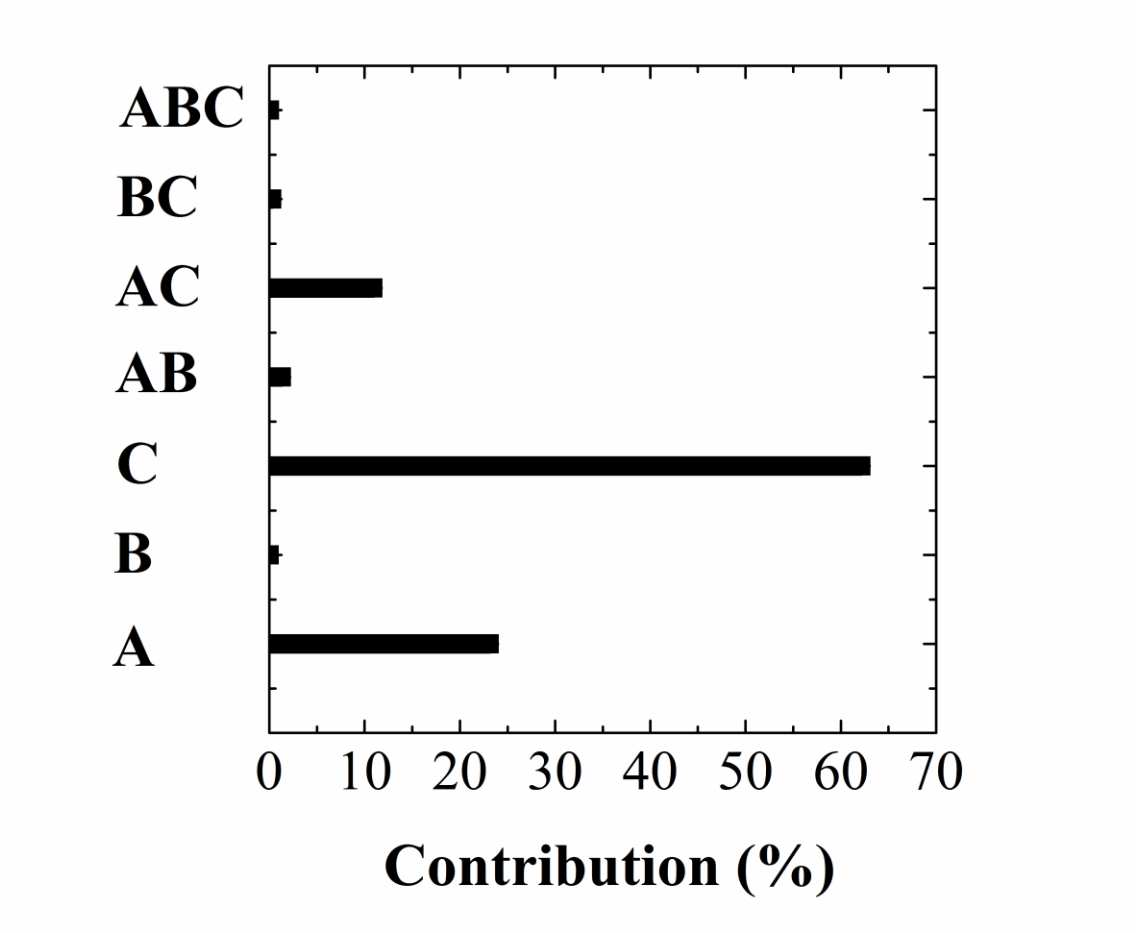

Figure 8. Contribution percentages of the process variables to the duration of the atmospheric freeze-drying of apple samples (A: temperature; B: air velocity; C: acoustic power).